Comparative analysis of two liner acoustic impedance characterization techniques

Victor Lafont, Rémi Roncen, Jérémie Derré, Florent Mercat

25·29 August 2024
inter.noise
NANTES FRANCE

Comparative analysis of two liner acoustic impedance characterization techniques

Victor Lafont[1], Rémi Roncen[2]
DMPE, ONERA, Université de Toulouse
31000 Toulouse, France

Jérémie Derré[3], Florent Mercat[4]
Acoustic testing team, Flight test and integration center, Airbus Operations SAS
316 route de Bayonne, 31060 Toulouse Cedex 09, France

ABSTRACT

This study presents the comparison of two methodologies of small size liner acoustic impedance characterization. The first one is based on a normal incidence broadband acoustic excitation up to 160 dB inside a 30-mm diameter circular tube, and uses the two microphones method, with microphones flush-mounted inside the waveguide. This bench, called NTMM and developed at Airbus, allows to directly compute the acoustic impedance at the surface of the sample. The second one lies on a measurement inside the B2A wind tunnel at ONERA, where the sample is mounted as one of the vein walls, leading to a grazing aero-acoustic excitation, up to Mach 0.3 and 155 dB with a broadband excitation. The impedance is then educed by an inverse method. During the MAMBO research project, dedicated samples have been designed and tested with the two benches as well as on the CANNELLE multimodal test rig developed by Airbus.

1. INTRODUCTION

Engine noise is the main contributor to overall aircraft noise, particularly during take-off. Over the last decades, the aviation industry has been consistently using acoustic liners within the propulsion system nacelle to mitigate fan noise transmission through the inlet and thrust reverser, making them the most effective noise reduction technology. Typical liners behave on a resonator principle, and are composed of a perforated plate, facing the flow, backed by a cavity controlling the resonance frequency of the system. The geometry of the cavity and perforated plate can be optimized to match specific noise damping requirements [1]. Acoustic liners are usually characterized by their surface impedance, a physical quantity relating the acoustic pressure and velocity at the homogenized surface of the sample.

To enhance liner efficiency, ongoing research explores novel acoustic liner technologies not limited to the simple single degree of freedom (SDOF) liners, with solutions tailored to match

[1]victor.lafont@onera.fr
[2]remi.roncen@onera.fr
[3]jeremie.derre@airbus.com
[4]florent.mercat@airbus.com

the noise profiles of modern engine fans, which typically display tones at lower frequencies than before, as well as solutions aimed at mitigating the effects of grazing flow [2–5].

Guess [6] provided a basis for perforated liners impedance prediction. Since then, multiple milestones were achieved, in particular regarding the modelling of flow effects and boundary layer effects [7–9], the knowledge of influence of the sound pressure level (SPL) on the nonlinear response of the liner [10, 11], as well as regarding impedance eduction methods [12–17].

Within the MAMBO DGAC project, the followed approach involves conducting a comprehensive benchmarking exercise across various laboratory impedance test benches and larger-scale facilities, simulating real-engine conditions. This project investigates impedance prediction methods and facilitates cross-comparison among the different test benches to validate these methodologies.

This paper aims to present initial comparisons between B2A and NTMM on select samples and offers an initial comparison with CANNELLE test results. Sections 2 and 3 describe the benches and methods used for the study, and Section 4 presents the main results obtained.

2. EXPERIMENTS

This section introduces the different experimental benches and acoustic liner samples used within the scope of this work.

2.1. Experimental benches

2.1.1. The NTMM test bench

The NTMM is an Airbus in-house impedance tube based on the two-microphone method (TMM) [18–20]. It follows the usual standards [21, 22] of similar test benches that can be found in many acoustic laboratories [23]. The cylindrical waveguide has a diameter of 30 mm and works in the plane-wave range for frequencies between 400 and 6000 Hz, at levels ranging from 110 to 160 dB. Two $^1/_4$-inch pressure-field microphones flush-mounted on the wall are used for measurements.

The dispersion and dissipation effects inside the duct are both considered, the latter being mainly driven by the wall viscothermal losses, modeled as in Ref. [24]. A flush-mounted sensor measures the fluid temperature in the duct, and is taken into account for the post-processing to accurately evaluate the speed of sound. Figure 1 presents an overview of the test rig.

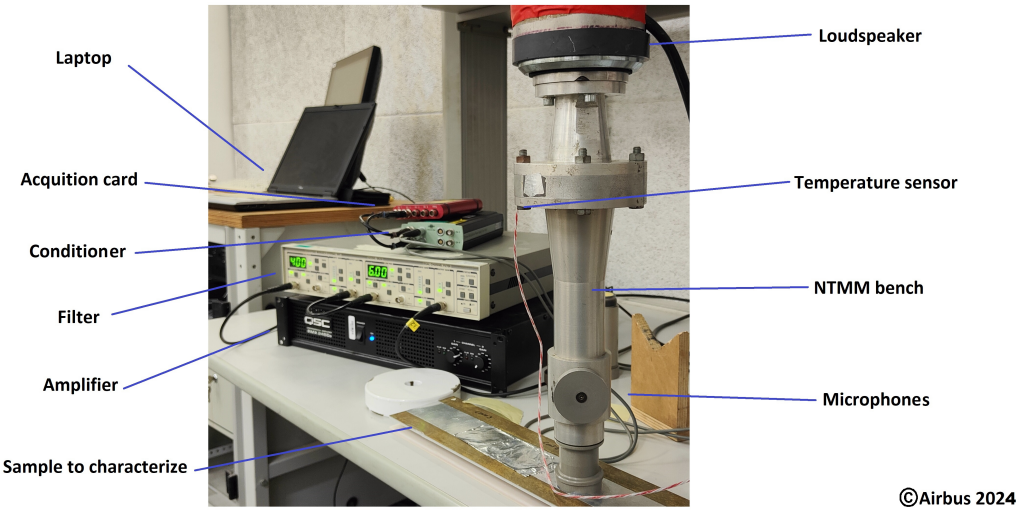

Figure 1: NTMM bench over a liner sample, with its generation and acquisition system

2.1.2. The B2A aeroacoustic bench

The B2A test bench (Figure 2) at ONERA is made of a tube with a square section of side $a = 50$ mm and a total length of about 4 m. A mean flow of bulk Mach number M_b up to 0.5 can be provided and its temperature can be accurately regulated from room temperature up to 570 K. In the duct, the flow is in a fully-developed turbulent state [25].

The test section is 200 mm long and is equipped with 17 microphone ports on its upper wall for acoustic pressure measurements. The liner samples are located on the lower wall of the test section and are 150 mm in length and 50 mm in width, spanning the whole duct width. Two speakers placed upstream of the test section are used to generate the acoustic excitation at levels up to 155 dB over a frequency range of 0.3 to 3.5 kHz. Since the maximum frequency used is below the cut-off frequency of the duct, all measurements and analyses are performed under the assumption that only plane waves propagate. The duct ends with an exponential anechoic outlet, ensuring a reflection coefficient lower than 0.2 across all frequencies of interest. More details on the B2A can be found in previous papers [26, 27].

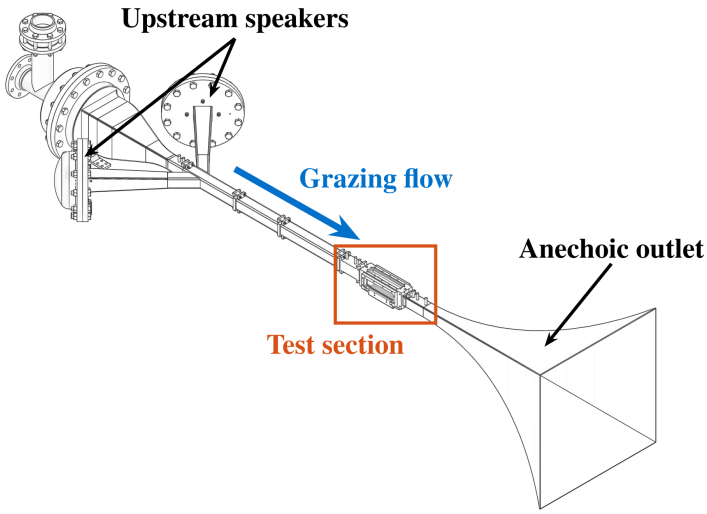

Figure 2: Sketch of the B2A bench

2.2. Liner samples

Three test samples are considered in this study. The first one is a standard SDOF acoustic liner, of 13 mm cell depth with a resistive sheet made of a wiremesh combined with a perforated composite plate (Figure 3a). The second one is a 3D-printed sample representative of an Airbus technology. This sample has a total height of about 50 mm, including a 1-mm thick perforated resistive plate of about 8 POA (Percent of Open Area) (Figure 3b). The last sample is a 3D-printed sample representative of an ONERA metasurface technology, including a 50 mm×50 mm pattern, with 3×3 cells of different height and POA, reproduced all along the sample. This sample has a total height of about 65 mm, and its flow-facing element includes a perforated sheet backed by a wiremesh. Photos of the samples are given in Figure 3, and a crude schematics of each technology is given in Figure 4 (schematics are not to scale, and proportions are not kept). Table 1 summarizes the main features of these acoustic liner samples.

Table 1: Geometry of the liner samples

Sample	Total depth (mm)	Face sheet POA
SDOFw	13	22
Airbus Techno	50	8
ONERA Techno	65	25.8

(a) SDOF sample with wiremesh face sheet

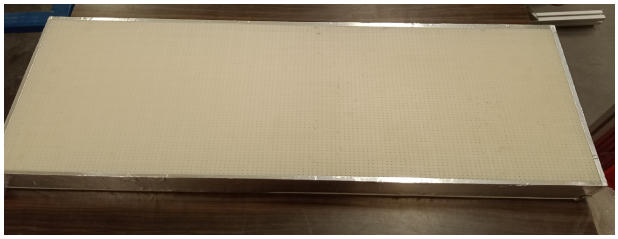

(b) Airbus Technology sample

(c) Onera Technology sample

Figure 3: Photographs of the different liner technologies involved in the project.

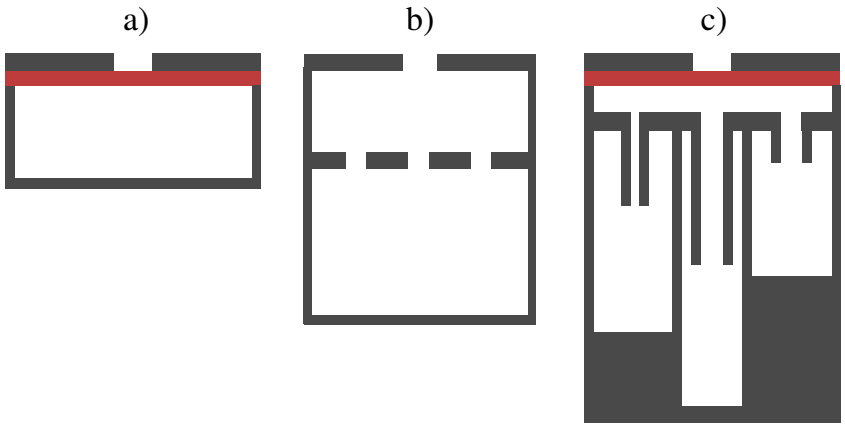

Figure 4: Schematics of the different liner technologies involved in the project. a) The SDOF sample with a facesheet backed by a wiremesh (red element). b) Airbus technology sample, DDOF-like behaviour. c) ONERA sample, with a perforated plate backed by a wiremesh, a small cavity, and an array of 3×3 cells containing extended neck resonators (LEONAR technology [2, 28]).

3. IMPEDANCE MEASUREMENTS

This section details the two approaches followed in this work to evaluate the surface impedance of the acoustic samples. The first one, used in the NTMM, is a direct approach, relying on the measurement of the acoustic pressure at two locations, with a normal wave incidence to the sample. The second one, used in the B2A, relies on an indirect approach based on the measurement of the acoustic pressure at 17 locations, with a grazing wave incidence to the samples.

3.1. In the NTMM: direct approach

The direct approach used in NTMM relies on a formulation equivalent to the one developed in Ref. [21]. In order to simplify the formulation and better answer the need, the material surface is used as the spatial origin to determine the acoustic pressure P_1 and P_2 at each microphone and their transfer function H_{12}, as

$$\begin{aligned} P_1 &= Ae^{-\mathrm{j}kl} + Be^{\mathrm{j}kl}, \\ P_2 &= Ae^{-\mathrm{j}k(l+d)} + Be^{\mathrm{j}k(l+d)}, \end{aligned} \tag{1}$$

with k the wave number, l the distance between the material surface and the first microphone, d the distance between the two microphones and

$$\begin{aligned} A &= \mathrm{j}P_1 \frac{H_{12}e^{\mathrm{j}kl} - e^{\mathrm{j}k(l+d)}}{2\sin(kd)}, \\ B &= \mathrm{j}P_1 \frac{e^{-\mathrm{j}k(l+d)} - H_{12}e^{-\mathrm{j}kl}}{2\sin(kd)}, \\ H_{12} &= \frac{P_2}{P_1}. \end{aligned} \tag{2}$$

Finally the reduced surface impedance of the sample is given by:

$$Z = \frac{A+B}{A-B}. \tag{3}$$

The NTMM method is limited to the study of plane waves, thus with upper operating frequency linked to the tube diameter. In addition, in order to avoid any evanescent mode measured at both microphones, a distance of at least one diameter is secured between material surface and first microphone, as well as between noise source and second microphone [21, 22].

Dissipation phenomena caused by visco-thermal effects along the duct are modeled in the NTMM using propagation constant k integrating viscous effects [24]:

$$k = k_0\left(1 + \frac{1}{\mathrm{Sh}}\frac{1-\mathrm{j}}{\sqrt{2}}\left(1 + \frac{\gamma-1}{\sqrt{\mathrm{Pr}}}\right)\right), \tag{4}$$

with k_0 the wavenumber, $\mathrm{Sh} = a\sqrt{\omega/\nu}$ the shear number, a the tube radius, $\mathrm{Pr} = 0.71$ the Prandtl number, $\nu = 1.51.10^{-5} + 9.2.10^{-8}(T-293.15)$ the kinematic viscosity, and $\gamma = 1.402$ the specific ratio of gas.

3.2. In the B2A: inverse approach

The impedance Z of liner samples is determined with an inverse eduction method based on the 2D linearized Euler equations (LEE). An assumed impedance is used in the LEE equations to determine acoustic pressures at the microphone locations (Figure 5). These pressures are then compared to the experimental results in an iterative scheme until the error between the two is minimized. The optimization process is carried out using the reflection coefficient instead of the impedance, as this coefficient is properly bounded on the complex unit disk.

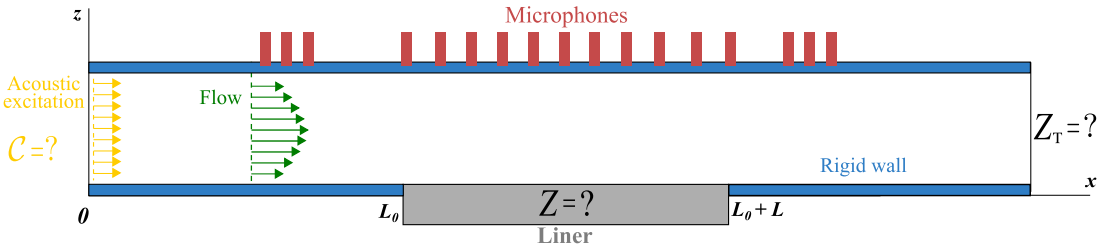

Figure 5: Impedance eduction in the B2A bench

The numerical resolution is done with a discontinuous Galerkin (DG) scheme, accounting naturally for the presence of a shear grazing flow in the simulation [14, 27].

The acoustic excitation used for the current study is a broadband white noise with an overall incident SPL equal to 140 dB. The incident SPL is determined using a two-microphone decomposition method [19, 26].

4. RESULTS

This section presents a comparison of the results obtained on the two small-scale benches described in Section 2, as well as early comparisons between grazing incidence measurements on the B2A bench and the larger-scale bench CANNELLE.

4.1. Impedance measurements

Figures 6 and 7 show the impedance results obtained on both benches for the first two samples. In the case of the B2A measurement, only the case without grazing flow is shown. For both samples, NTMM and B2A results seem to agree quite well for similar SPLs.

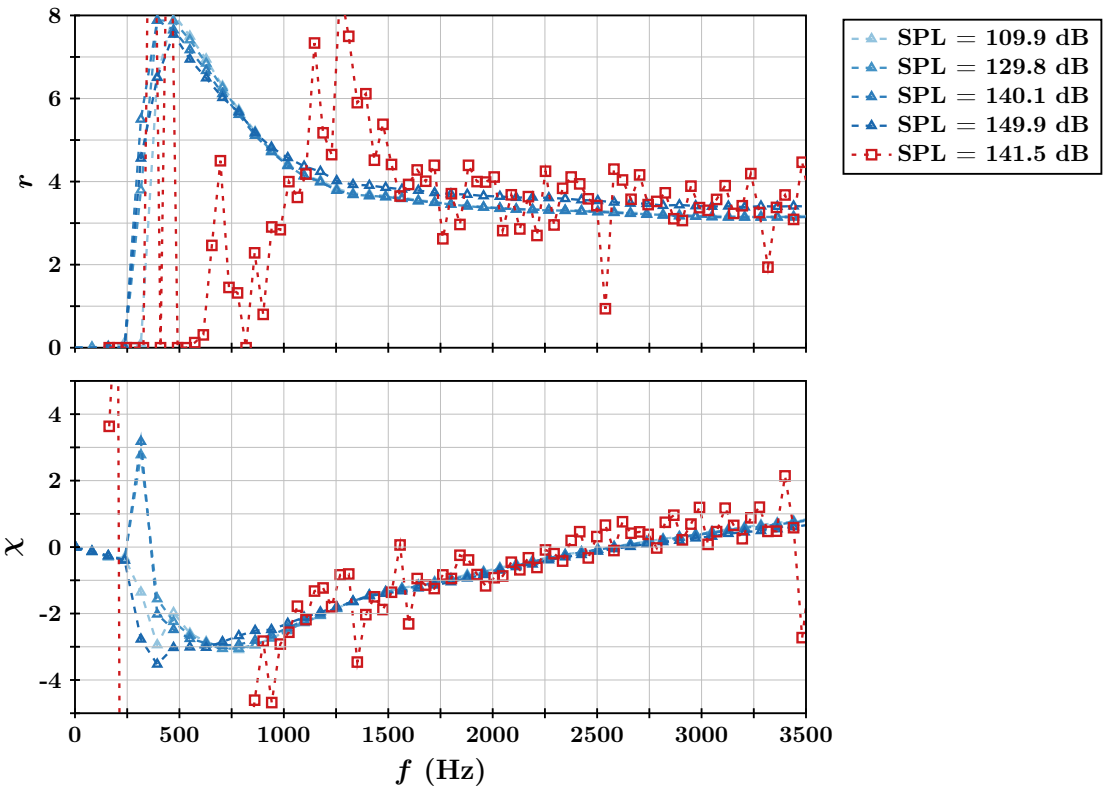

Figure 6: Comparison of impedances obtained with the NTMM (blue curves) and with the B2A bench without grazing flow (red curves), SDOF liner with wiremesh.

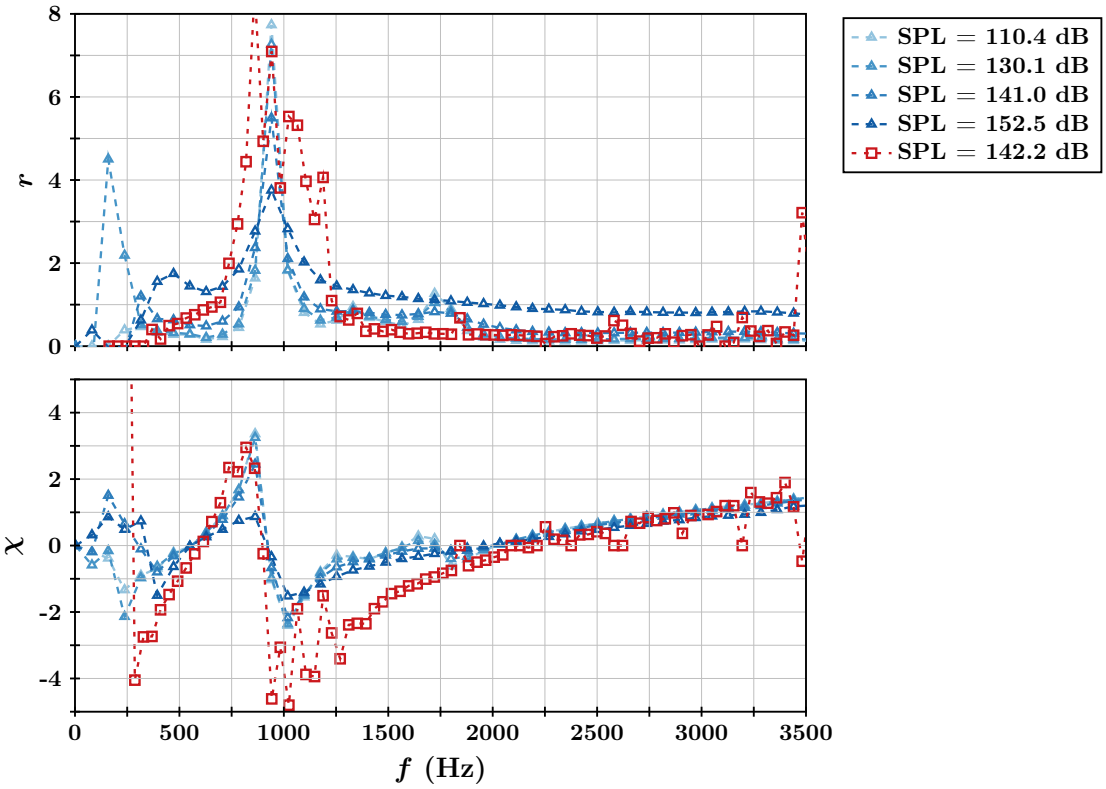

Figure 7: Comparison of impedances obtained with the NTMM (blue curves) and with the B2A bench without grazing flow (red curves), Airbus liner.

The NTMM method is non-destructive, applying the tube directly on a surface greater than the one of the tube itself. consequently, some leakage can appear and affect behaviour at low-frequency, as can be observed in Figure 6 up to 750Hz.

The first liner design appears quite insensitive to the incident SPL. As shown by the NTMM measurements, this sample has a quite high resistance. Since the associated reflection coefficient is close to 1, small uncertainties on its value during the eduction process might lead to unusually large variations on the educed impedance, which makes it difficult to obtain a "true" impedance value and explains the noisy results and the discrepancies observed at low frequencies on the B2A results. Future work will focus on improving the stability of the eduction algorithm in such highly reflective cases.

For the second design, the double resonance induced by the DDOF-like behaviour appears clearly, with a first resonant frequency around 700 Hz and a second one around 2 kHz. As for the first design, the resistance is not affected much by the changes in incident SPL. The reactance measured on this sample with the NTMM bench has a flatter shape than the reactance measured with the B2A, especially at high SPL: this is mainly due to increased viscous effects.

The third sample with multiple cavities and added facesheet and wiremesh was not tested in the NTMM bench due to size constraints. Some impedance eduction results on this liner design are presented in Ref. [29].

4.2. Absorption and TL comparisons in a different duct

In the frame of the MAMBO project, a measurement campaign on a larger-scale test rig named CANNELLE was also performed. CANNELLE is a test bench developed by Airbus aiming at characterizing acoustic liner barrels in conditions more representative of an engine during flight [30]. It has a circular cross-section and is composed of several modular parts (see Figure 8). A generation section with 50 loudspeakers allows acoustic generation with control of the generated azimuthal mode and an SPL up to 150 dB; two other sections placed around the liner section and called detection barrels allow modal detection and decomposition thanks to 150 flush-mounted microphones on each section. The test section itself can accommodate liner barrels with a treated length of 350 mm.

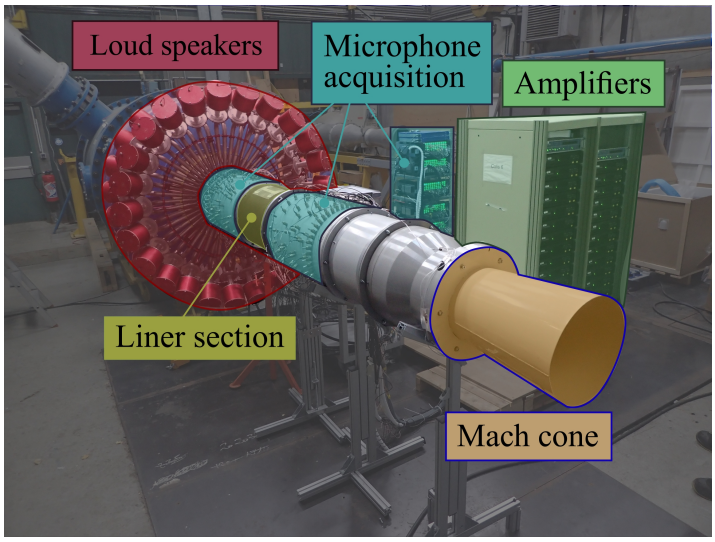

Figure 8: CANNELLE test bench in ONERA R4 wind-tunnel

The rig can be used either in a static condition (no grazing flow) or with a grazing flow up to Mach 0.6 when plugged to the ONERA R4 facility. In that case, the loudspeaker section can be mounted upstream or downstream of the test section and detection barrels to simulate either a bypass duct configuration or a nacelle inlet environment, with acoustic waves travelling respectively with or against the flow. The flow is regulated by placing specific sonic throats at the end of the duct for each desired speed; this method also ensures downstream acoustic anechoicity.

Several liner barrels, representative of the flat liner samples tested on the B2A and NTMM benches, were fabricated for the measurement campaign. A first comparison in static condition is presented here, deeper analysis is currently in progress on tests with flow.

Figures 9 to 11 show a comparison of the acoustic behaviour of the three considered samples in the B2A bench and in the CANNELLE test rig. The green curve is a transmission loss (TL) measurement, without grazing flow, obtained in the B2A bench at an incident SPL of 140 dB. The blue squares, circles and triangles correspond to the TL measured in the CANNELLE rig for acoustic azimuthal modes 0, 1 and 2 respectively.

Since the geometries of the two benches differ greatly, the TL values have no reason to be identical: this comparison aims only at providing a first basis for further analysis of the CANNELLE measurements. For the three liner barrels, the shapes of the TL measured with the CANNELLE setup and in the B2A configuration on the corresponding flat small-scale samples are quite similar. The broadband absorption capacity of the ONERA liner appears clearly as the TL is over 5 dB everywhere, while the Airbus design presents a DDOF-like response, with two main TL peaks. The SDOF with wiremesh sample also has a quite wide absorption range, with TL increasing near the higher frequencies, close to its expected resonance.

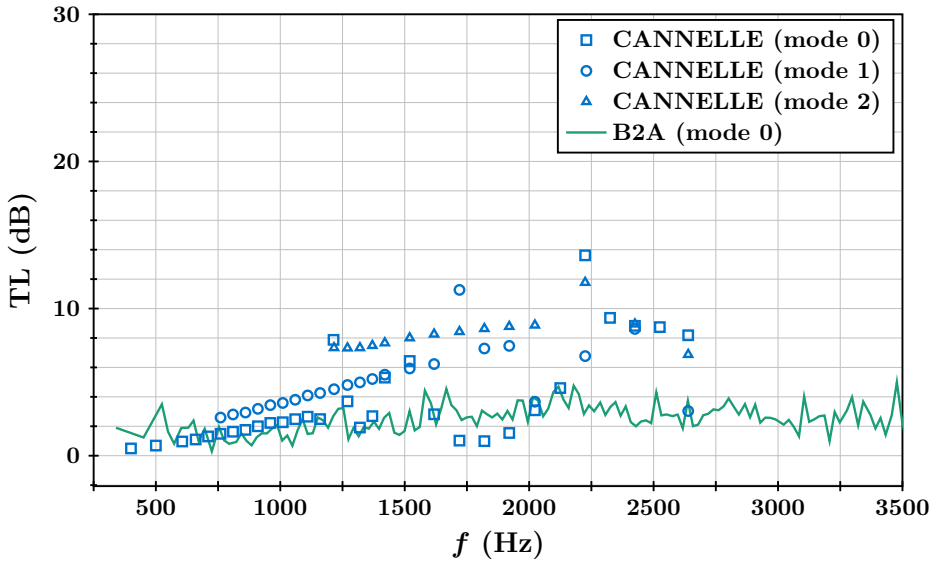

Figure 9: Comparison of the TL obtained in the B2A bench (green solid line) and in CANNELLE without flow (blue markers), SDOF liner barrel.

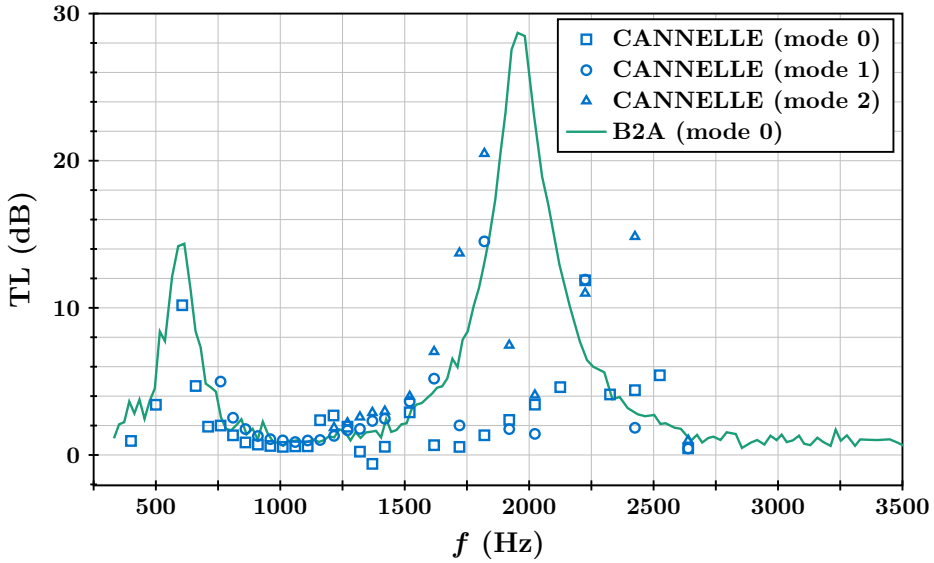

Figure 10: Comparison of the TL obtained in the B2A bench (green solid line) and in CANNELLE without flow (blue markers), Airbus liner barrel.

5. CONCLUSIONS

The study focuses on a comparison between two methodologies for characterizing small-sized liner acoustic impedance: the NTMM (normal incidence tube with the two-microphone method) developed at Airbus and the B2A wind tunnel at ONERA. The NTMM uses a normal incidence broadband acoustic excitation within a portable cylindrical waveguide, allowing for direct computation of acoustic impedance at the surface of the sample. On the other hand, the B2A bench employs a grazing aero-acoustic excitation in a square-sectioned tube, with the impedance educed through an inverse method based on the linearized Euler equations and a minimization algorithm. In addition, a third larger bench was used, the CANNELLE test rig.

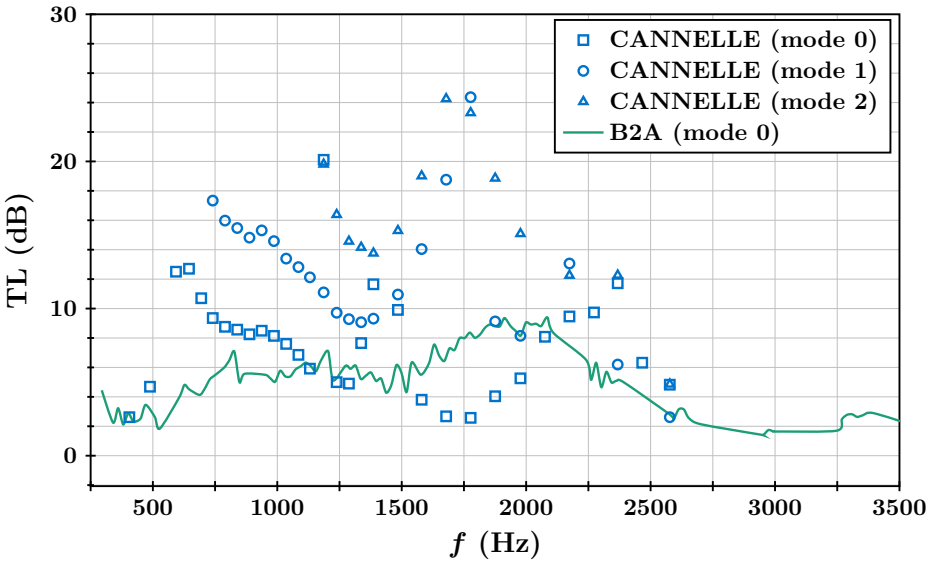

Figure 11: Comparison of the TL obtained in the B2A bench (green solid line) and in CANNELLE without flow (blue markers), ONERA liner barrel.

Experiments were conducted with dedicated samples tested on two or more benches. Two samples were considered first in both the NTMM and B2A benches: a standard SDOF liner with a wiremesh, and an Airbus technology sample with DDOF-like behaviour. An additional liner based on an ONERA technology, featuring multiple cavities and extended resonators, was tested in both the B2A and CANNELLE test benches. The impedance measurements obtained from the NTMM and B2A benches showed good agreement for similar SPLs. Discrepancies were observed in cases of highly resistant samples, where the B2A measurements exhibited variations which the authors believe to be due to difficulties in impedance eduction for highly resistive samples; future work on the impedance eduction process used with the B2A bench will focus on overcoming these difficulties.

Initial comparisons in static conditions of the CANNELLE bench revealed promising correlations between absorption coefficients obtained from NTMM and B2A impedance measurements, and transmission loss (TL) obtained from CANNELLE tests. The next steps relate to the post-treatment of the CANNELLE test campaign, which includes experiments with flows up to Mach 0.6 on the different liner technologies, on a wide frequency spectrum and with up to 50 passing modes. Numerical simulations will complement this analysis to try and educe the impedance directly from the data obtained in the CANNELLE measurement rigs, to obtain a more complete comparison between benches and quantify the sources of uncertainties in liner design and manufacturing within these types of experimental campaigns.

ACKNOWLEDGEMENTS

This work was carried out in the framework of the MAMBO project, supported by the French Civil Aviation Agency (DGAC) under DGAC Convention 2021-50, the "France Relance" national recovery plan, and the "Nextgeneration EU" European recovery plan. Estelle Piot is warmly acknowledged for the helpful discussions on the uncertainties in the impedance eduction process.

REFERENCES

1. R. Motsinger and R. Kraft. Design and performance of duct acoustic treatment. *Aeroacoustics of Flight Vehicles: Theory and Practice. Volume 2: Noise Control*, 1991.
2. M. G. Jones, F. Simon, and R. Roncen. Broadband and low-frequency acoustic liner investigations at NASA and ONERA. *AIAA Journal*, 60(4):2481–2500, 2022.
3. C. Yang, P. Zhang, S. Jacob, E. Trigell, and M. Åbom. Investigation of extended-tube liners for control of low-frequency duct noise. *AIAA Journal*, 59(10):4179–4194, 2021.
4. J. Guo, Y. Fang, Z. Jiang, and X. Zhang. An investigation on noise attenuation by acoustic liner constructed by Helmholtz resonators with extended necks. *The Journal of the Acoustical Society of America*, 149(1):70–81, 2021.
5. Y. Murata, T. Ishii, S. Enomoto, H. Oinuma, K. Nagai, J. Oki, and H. Daiguji. Experimental research on new acoustic liners combined with fine-perforated-film. In *28th AIAA/CEAS Aeroacoustics 2022 Conference*, page 2885, 2022.
6. A. Guess. Calculation of perforated plate liner parameters from specified acoustic resistance and reactance. *Journal of Sound and Vibration, vol. 40, no. 1*, page 119–137, 1975.
7. M. K. Myers. On the acoustic boundary condition in the presence of flow. *Journal of Sound and Vibration, Vol. 71,No. 3*, page 429–434, 1980.
8. E. Brambley. A well-posed modified Myers boundary condition. *16th AIAA/CEAS Aeroacoustics Conference*, 2010.
9. Y. Aurégan and Y. Renou. Failure of the Ingard–Myers boundary condition for a lined duct: An experimental investigation. *J. Acoust. Soc. Am. 130*, page 52–60, 2011.
10. T. H. Melling. The acoustic impendance of perforates at medium and high sound pressure levels. *J. Sound Vib.*, 29(1):1–65, 1973.
11. M. A. Temiz, J. Tournadre, I. L. Arteaga, and A. Hirschberg. Non-linear acoustic transfer impedance of micro-perforated plates with circular orifices. *Journal of Sound and Vibration*, 366:418–428, 2016.
12. X. Jing, S. Peng, and X. Sun. A straightforward method for wall impedance eduction in a flow duct. *The Journal of the Acoustical Society of America*, 124(1):227–234, 2008.
13. W. R. Watson and M. G. Jones. A comparative study of four impedance eduction methodologies using several test liners. In *19th AIAA/CEAS Aeroacoustics Conference*, page 2274, 2013.
14. J. Primus, E. Piot, and F. Simon. An adjoint-based method for liner impedance eduction: Validation and numerical investigation. *Journal of Sound and Vibration*, 332(1):58–75, 2013.
15. C. Weng, A. Schulz, D. Ronneberger, L. Enghardt, and F. Bake. Flow and viscous effects on impedance eduction. *AIAA Journal*, 56(3):1118–1132, 2017.
16. R. Roncen, F. Méry, E. Piot, and F. Simon. Statistical inference method for liner impedance eduction with a shear grazing flow. *AIAA Journal*, 57(3):1055–1065, Mar. 2019.
17. M. G. Jones and B. M. Howerton. Benchmark data for evaluation of NASA impedance eduction methods. *AIAA AVIATION 2021 FORUM*, 2021.
18. J. Derré, M. Gomes, N. Sauron, and T. Abily. Perforation ratio evaluation of liner treatments by experimental approaches with acoustical and optical methods. In *Forum Acusticum 2023*, Torino, Italy, Sept. 2023.
19. J. Y. Chung and D. A. Blaser. Transfer function method of measuring in-duct acoustic properties. I. Theory. *The Journal of the Acoustical Society of America*, 68(3):907–913, 1980.
20. J. Y. Chung and D. A. Blaser. Transfer function method of measuring in-duct acoustic properties. II. Experiment. *The Journal of the Acoustical Society of America*, 68(3):914–921, 1980.

21. ISO 10534-2:1998. *Acoustics - Determination of sound absorption coefficient and impedance in impedance tubes - Part 2: transfer-function method.* International Organization for Standardization, Geneva, Switzerland, 1998.
22. ASTM E1050-08. *Standard Test Method for Impedance and Absorption of Acoustical Materials Using a Tube, Two Microphones and a Digital Frequency Analysis System.* ASTM International, 2008.
23. T. Schultz, F. Liu, L. Cattafesta, M. Sheplak, and M. Jones. Comparison study of normal-incident acoustic impedance measurements of a perforate liner. In *15th AIAA/CEAS Aeroacoustics Conference (30th AIAA Aeroacoustics Conference)*, page 3301, 2009.
24. M. Bruneau. *Fundamentals of Acoustics.* Lavoisier, 2006.
25. O. Léon, F. Méry, E. Piot, and C. Conte. Near-wall aerodynamic response of an acoustic liner to harmonic excitation with grazing flow. *Experiments in Fluids*, 60(9):144, Aug. 2019.
26. F. Méry, E. Piot, D. Sebbane, P. Reulet, F. Simon, and A. Carazo Méndez. Experimental assessment of the effect of temperature gradient across an aeroacoustic liner. *Journal of Aircraft*, 56(5):1809–1821, 2019.
27. V. Lafont, F. Méry, R. Roncen, F. Simon, and E. Piot. Liner impedance eduction under shear grazing flow at a high sound pressure level. *AIAA Journal*, 58(3):1107–1117, 2020.
28. F. Simon. Long Elastic Open Neck Acoustic Resonator for low frequency absorption. *Journal of Sound and Vibration*, 421:1–16, 2018.
29. V. Lafont, R. Roncen, F. Méry, and D. Sebbane. Evaluation of a metasurface liner concept for broadband acoustic absorption. In *Forum Acusticum 2023*, Torino, Italy, Sept. 2023.
30. M. Lavieille and S. Le-Saint. Impedance eduction of liners in no-flow condition and based on multimodal excitation. In *23rd AIAA/CEAS Aeroacoustics Conference*, page 3180, 2017.